Archives of Razi Institute, Vol. 76, No. 3 (2021) 571-586

Copyright © 2021 by
Razi Vaccine & Serum Research Institute
DOI: 10.22092/ari.2020.342702.1477

Original Article

A New Amphotericin B-loaded Trimethyl Chitosan Nanoparticles as a Drug Delivery System and Antifungal Activity on *Candida albicans* Biofilm

Nemati Shizari, L[1], Mohammadpour Dounighi, N[2] *, Bayat, M[1], Mosavari, N[3]

1. Department of Microbiology, Medical and Veterinary Mycology, Faculty of Veterinary Specialized Science, Science and Research Branch, Islamic Azad University, Tehran, Iran
2. Department of Human Vaccine and Serum, Razi Vaccine and Serum Research Institute, Agricultural Research, Education and Extension Organization (AREEO), Karaj, Iran
3. Department of Tuberculosis, Razi Vaccine and Serum Research Institute, Agricultural Research, Education and Extension Organization (AREEO), Karaj, Iran

Received 22 April 2020; Accepted 5 July 2020
Corresponding Author: nasser_mohammadpour@yahoo.com

Abstract

Amphotericin B (AmB) is an effective antifungal agent; however, the application of AmB is associated with a number of drawbacks. Application of nanoparticles (NPs) is known to improve the efficiency of drug delivery to the target tissues, compared to the traditional methods. In this study, a novel method of NPs preparation was developed. The trimethyl chitosan (TMC) was synthesized using low molecular weight chitosan and was used for the preparation of TMC-NPs through ionic gelation method. Afterward, AmB-loaded TMC-NPs (TMC-NPs/AmB) were prepared and their drug delivery potential was testes. The TMC-NPs and TMC-NPs/AmB were characterized for their structure, particle size, Zeta potential, polydispersity index, morphology, loading efficiency, loading capacity, *in vitro* release profile, release kinetic, and entrapped AmB potency. The cytotoxicity and antifungal activity of TMC-NPs/AmB against Candida albicans biofilm were evaluated. The quaternization of TMC was estimated to be 36.4%. The mean particle size of TMC-NPs and TMC NPs/AmB were 210±15 and 365±10 nm, respectively, with a PDI of 0.30 and 0.4, ZP of +34±0.5 and +28±0.5 mV, respectively. Electron microscopy analysis indicated uniform spherical shapes with smooth surfaces. The TMC-NPs/AmB indicated LE of 76% and LC of 74.04 % with a potency of 110%. The release profile of TMC-NPs/AmB was best explained by the Higuchi model. The initial release after 10 h was obtained at 38%, and the rates of release after 36 and 84 h were determined at 67% and 76% respectively, which was significantly different ($P<0.05$) from previous time points. The minimum inhibitory concentration (MIC) (50%) of NPs/AmB and AmB were 0.65 and 1.75 µg/mL, and the MIC 80% were determined at 1.95 and 7.75 µg/mL, respectively, demonstrating a significant improvement in antifungal activity. The half-maximal inhibitory concentration for TMC-NPs/AmB and AmB were estimated at 86 and 105 µg/mL, respectively, indicating a significant reduction in cytotoxicity and the adverse effect. This study could successfully introduce a practical method to synthesize TMC-NPs. The encapsulation process was efficient and significantly improved the antifungal activity of AmB. The developed method can be applied to improve the feasibility of oral delivery while reducing the adverse effects associated with traditional methods.

Keywords: Amphotericin B; Nanoparticles; Trimethyl Chitosan; Candida albicans; Biofilm

Un Nouveau Amphotéricine B Chargé de Nanoparticules de Triméthyl Chitosan Comme Système D'administration de Médicaments et Activité Antifongique sur le Biofilm de *Candida albicans*

Résumé: L'amphotéricine B (AmB) est un agent antifongique efficace. Cependant, l'application d'AmB est associée à un certain nombre d'inconvénients et d'effets secondaires. L'application de nanoparticules (NPs) est

connue pour permettre une administration de médicament plus efficace aux tissus cibles que les méthodes traditionnelles. Dans cette étude, le triméthyl chitosan (TMC) a été synthétisé à partir de chitosan de bas poids moléculaire. Le TMC a ensuite été utilisé pour la préparation de TMC-NPs par la méthode de gélification ionique. Ensuite, des TMC-NPs chargés en AmB (TMC-NPs/AmB) ont été préparés et leur application potentielle pour l'administration de médicaments. Les TMC-NPs et TMC-NPs /AmB ont été caractérisés pour leur structure, la taille des particules, le potentiel zêta (PZ), l'indice de polydispersité (IPD), la morphologie, l'efficacité de chargement (EC), la capacité de charge (LC), le profil de libération in vitro, libérer la puissance cinétique et piégée d'AmB. Ensuite, la cytotoxicité et l'activité antifongique des TMC-NPs/ AmB contre le biofilm de Candida albicans ont été évaluées. Dans cette étude, le pourcentage de quaternisation de TMC est estimé à 36.4. La taille moyenne des particules de TMC-NPs et TMC NPs/AmB était respectivement de 210±15 et 365±10 nm, avec un IPD de 0.30 et 0.40, ZP de +34± 0.5 et +28±0.5 mV respectivement. L'analyse au microscope électronique a indiqué des formes sphériques uniformes avec des surfaces lisses. Le TMC-NPs/AmB a indiqué EC de 76% et LC de 74.04% avec une puissance de 110%. Le profil de libération des TMC-NPs/AmB a été mieux expliqué par le modèle Higuchi. La libération initiale après 10 h était de 38% et le taux de libération après 36 et 84 h était de 67% et 76% respectivement, ce qui était significativement différent ($P<0.05$) des points de temps précédents. La concentration minimale inhibitrice (CMI) à 50% des NPs/AmB et AmB était de 0.65 et 1.75 µg/mL et la CMI de 80% était de 1.95 et 7.75 µg/mL, démontrant respectivement une amélioration significative de l'activité antifongique. La demi-concentration inhibitrice maximale pour les TMC-NPs/AmB et AmB était de 86 et 105 µg/mL respectivement, indiquant une réduction significative de la cytotoxicité et de l'effet indésirable. Cette étude pourrait introduire avec succès une méthode pratique pour synthétiser un TMC-NPs. Le processus d'encapsulation a été efficace et a considérablement amélioré l'activité antifongique de l'AmB. La méthode développée peut être appliquée pour améliorer la faisabilité de l'administration orale tout en réduisant les effets indésirables associés aux méthodes traditionnelles.

Mots-clés: Amphotéricine B; Nanoparticules; Triméthyl chitosane; Candida albicans; Biofilm

1. Introduction

Amphotericin B (AmB) is a broad-spectrum antifungal medicine used for the treatment of invasive fungal infections and leishmaniasis (1). For decades, AmB has been known as the “gold standard” for curing most fungal infections (2). AmB causes intracellular cation leakage by combining ergosterol on the fungal cell membrane that leads to cell death by impairing the cell membrane permeability (3).

Fungal pathogens, such as Candida species are known for their ability to form a biofilm that is associated with multidrug resistance and poor clinical outcomes (4). In comparison with other antifungal medicines, such as azoles, AmB has been proved to be more effective in controlling and treatment of life-treating systematic fungal infection; moreover, it has been subjected to a lesser degree of antifungal resistance in patients infected with biofilm proficient strains (1).

The AmB is generally administrated in high total doses due to its poor water solubility and limited oral absorption (3). Application of high doses of AmB is associated with several dose-dependent side effects, such as nephrotoxicity including renal vasoconstriction and decreased glomerular filtration rate that may result in permanent loss of renal function (5). Despite its efficiency in the treatment of severe systematic fungal infection, it is not the first-line treatment due to its limitations (3).

Significant efforts have been undertaken to improve the bioavailability of AmB through the application of various drug delivery methods. A number of sustained-release systems and drug careers, such as liposomes, dendrimers, and modified nanoparticles (NPs), have been examined to enhance the solubility rate and delivery of the drug to the target tissue (6). Chitosan-based NPs drug delivery system has been widely used to improve drug delivery to enhance the therapeutic efficacy of the drugs (1). Chitosan is an N-deacetylated derivative of natural chitin obtained from crustaceans. Chitosan and its derivatives are hydrophilic polymers with specific functional properties that make them an

ideal candidate to be applied as a drug career in sustained-release systems. Some of the main advantages of the application of Chitosan-based NPs are excellent biocompatibility, biodegradability, low toxicity, and good penetrability (7). In addition, chitosan exhibits natural antifungal properties that enhance the activity of the drug (8).

Insolubility in the alkaline mediums is one of the major limitations of chitosan applications for the group of drugs that are soluble in alkaline pH. To overcome this limitation, numerous attempts have been made to modify chitosan, such as PE-gelatination and carboxymethylation of chitosan (9). Trimethyl chitosan (TMC) is a quaternized chitosan derivative that has perfect water solubility in a wide range of pH (10). The TMC has demonstrated a better penetration and mucoadhesive property, compared to chitosan. These properties make TMC a good candidate to produce medicines that are soluble in basic-pH conditions. Therefore, this study aimed to develop a novel TMC-based NPs (TMC-NPs) formulation to improve AmB delivery performance by targeting particular organs, reducing the side effects of the traditional AmB medicine and total required dosage, as well as shortening the duration of antibiotic therapy.

2. Material and Methods

2.1. Chemicals

Low molecular weight Chitosan was supplied from Primex Company, Iceland. According to the manufacturer's specifications, the viscosity and the deacetylation degree (DD) were <20 cP (1% solution in 1% acetic acid) and ≥95%, respectively. The sodium tripolyphosphate (STPP), n-methyl-2-pyrrolidone (NMP), methyl iodide (MeI), potassium iodide, Dimethyl sulfoxide (DMSO), 3-(4,5-dimethylthiazol-2-yl)-2,5-diphenyltetrazolium bromide (MTT), and sodium deoxycholate (NaDC) were purchased from (Merck, Germany). Moreover, Sabouraud Dextrose Agar (SDA) and Sabouraud dextrose broth (SDB) were obtained from (Sigma-Aldrich, USA). It should be noted that 96-well polystyrene microplates were purchased from (Nunc, Denmark).

The AmB and AmB Reference Standard were provided from (Sigma-Aldrich, USA). The Vero cells ATCC L-81, *Saccharomyces cerevisiae* ATCC 9763, and *Candida albicans* ATCC 10231 as a freeze-dried vial were obtained from the Razi Vaccine and Serum Research Institute, Karaj, Iran. All other chemicals used in this study were of analytical grade.

2.2. Solutions and Buffers

In this study, the solution containing NaDC 5% weight by volume (W/V) and DMSO 0.06% volume/volume (V/V) p (H 7±0.5) as an AmB solvent buffer. The 0.2M potassium phosphate solution containing DMSO 5% V/V (pH 10.5) and the phosphate buffer saline (PBS) pH 7.4 as dilution buffers were utilized in this study.

2.3. Structural Analysis

Fourier transform infrared (FTIR) spectroscopy (PerkinElmer, RX I spectrophotometer, USA) was used to study the structure of chitosan and TMC. The FTIR spectra were prepared at wavenumbers ranging from 450-4000 cm^{-1} using a KBr disk technique at ambient temperature (11).

Proton nuclear magnetic resonance (^{1}H-NMR) spectrum of TMC was recorded to identify the hydrogen framework and determine the chitosan quatrization degree or methylation percentage (DQ%) in D2O using a 600 MHz spectrometer (Bruker-Biospin, Rheinstetten, Germany) at 80°C. The following equation was used for calculating DQ% in TMC DEW (12).

$DQ\% = [(CH3)_3]/ [H] \times 1.9 \times 100$

2.4. Synthesis of TMC

The TMC was synthesized according to the method developed by (9). Briefly, 2 g of chitosan powder (Primex, Iceland) was dissolved in 100 mL of n-methyl-2-pyrrolidone (NMP; Merck, Germany) as a solvent and stirred at room temperature for 18 h. Subsequently, 16 mL of NaOH (15% W/V) and 6 g of sodium iodide were added and stirred at 60°C for 15

min, followed by adding 16 mL of MeI in three steps with three-hour intervals. They were then placed in a shaking water bath (60°C, 24 h) (THERMOLAB, GLF, Germany). The product was precipitated from the solution by 1200 mL of acetone to obtain a powdery substance, which is TMC iodide.

Final products were washed with acetone to replace the iodide-ion with chloride-ion. In the next step, they were dissolved in 80 mL of NaCl (10% W/V) to remove impurities. The product was precipitated using ethanol and centrifugation. The solution was then dialyzed against Triple-distilled deionized water for three days. The polymer was freeze-dried and milled to obtain an off-white water-soluble powder.

2.5. AmB Assay

In this study, the spectrophotometric method was used for quantifying AmB (Analytik Jena Specord 250 UV/Vis, Germany) (13). Briefly, the absorption spectra of AmB (0.0005% W/V in AmB solvent) were recorded at wavelength 200-900 nm, and the λ_{max} was then determined. The standard curve of different concentrations of AmB solution (AmB-sol) absorption in the λ_{max} was prepared and used for drug concentration measurement during the study.

2.6. Preparation of TMC-NPs

The TMC-NPs and AmB-loaded TMC-NPs (TMC-NPs/AmB) were prepared using the ionic gelation method (14). The effects of different concentrations of TMC (1.8 and 2 mg/mL) and sodium tripolyphosphate (STPP) (0.6, 0.75, and 1.0 mg/mL) in distilled water were examined and the optimum TMC-NPs construction conditions was estimated. In the optimized conditions, 4 mL of STPP solution (0.6 mg/mL) was added dropwise to 10 mL of TMC solution (1.8 mg) under magnetic stirring (1100 rpm, 25°C). Following that, TMC-NPs were centrifuged (13000g, 40 min) (Eppendorf, Centrifuge 5810 R, Hamburg, Germany), and the TMC-NPs were separated and analyzed for particle size, polydispersity index (PDI), and Zeta potential (ZP) by Zetasizer (Malvern Nano-ZS, UK), as well as surface and morphology using Field Emission Scanning Electron microscopy (SEM) (Hitachi S-4160, Japan).

2.7. Preparation of TMC-NPs/AmB

The TMC-NPs/AmB were fabricated by adding the STPP solution containing AmB-sol (125 µg/mL) to the TMC solution in optimum conditions achieved for synthesizing TMC-NPs. The TMC-NPs/AmB characterized for particle size, PDI, ZP, surface and morphology by SEM, loading efficiency (LE), loading capacity (LC), and in-vitro release profile (14, 15). The kinetics of drug release from NPs was performed based on five models of Zero order, First order, Hixon-Crowell, Higuchi, and Korsmeyer-Peppas models (16, 17). The LE of the drug in the TMC-NPs fabrication process and LC were calculated by following equations

$$LC(\%w/w) = \frac{\text{Total amount of drug} - \text{amount of drug in supernatant}}{\text{Total amount of formulation component}} \times 100$$

$$LE(\%w/w) = \frac{\text{Total amount of drug} - \text{amount of drug in supernatant}}{\text{Total amount of drug used}} \times 100$$

2.8. In-vitro Drug Release Study

For the *in vitro* release assessment of AmB from TMC-NPs/AmB, 1 mg/mL suspension of TMC-NPs/AmB was prepared in PBS, and the shaker was incubated at 170 rpm (25°C) (Orbital, GLF 3031, Germany). One-mL samples were taken at special time intervals after incubation at 0, 1, 2, 4, 6, 8, 10, 12, 24, 36, 48, 60, 72, and 86 h. Subsequently, the samples were centrifuged (65000g, 30 min), the concentration of Amb in the supernatant of each sample was measured, and percentage of drug released at different time intervals calculated in this study (18, 19).

2.9. Potency of AmB

The microbiological cylinder plate assay method was used according to the US Pharmacopeia for determination potency of AmB (20) The SDA culture medium was formulated using the meat peptone (9.4 g), yeast extract (4.7 g), beef extract (4.7 g), NaCl (10 g), dextrose (10 g), and agar (23.5 g) in 1-liter double distilled water (pH 6.1). The *Saccharomyces cerevisiae* ATCC 9763 (obtained as a freeze-dried vial from Razi

Vaccine and Serum Research Institute, Karaj, Iran) was cultured on SDA (30°C, 72 h), and the colonies organism were collected using sterile normal saline. Afterward, the density of microorganism suspension was adjusted by a spectrophotometer at 580 nm in 25% transmittance. Totally, five dilutions of 0.64, 1.80, 1.00, 1.25, and 1.56 µg/mL of the standard AmB (S_1-S_5) were prepared in dilution buffer. Moreover, a test solution AmB 1.00 µg/mL (equivalent to S3 of standard AmB) was prepared and named U3.

A total of three plates for each standard and the test solutions were selected in this study. The culture medium was prepared and mixed through the pour plate method with 1:100 yeast suspension at 40-45°C. In the next step, 8 mL of the final suspension was added to each plate, and then six cylinders were placed on each plate. A volume of 100 µL from the standard solutions and test solutions were poured in the three cylinders in each related plate, and the S3 was poured in solution in the next three cylinders. The plates were incubated (30°C, 48 h) and then the diameter (mm) of the growth inhibition zone was measured. The test was repeated three times, and calculations were made according to the standard protocol (20, 21).

2.10. Cytotoxicity Test

Cytotoxicity was determined by MTT colorimetric assay (14). Furthermore, the Vero cells ATCC L-81 (obtained as a freeze-dried vial from Razi Vaccine and Serum Research Institute, Karaj, Iran) were cultured in 96-well polystyrene microplates (Nunc, Denmark) at a seeding density of $3\text{-}4\times10^3$ cells per well. Subsequently, the AmB-sol and TMC-NPs/AmB were added in dilutions of 8 to 128 µg/mL, respectively. The control wells were treated by the drug-free medium. The MTT solution 0.005 g/mL was added to each well after 10 h of incubation (37°C, 5% CO2), and then the microplate was wrapped in aluminum foil and incubated (37°C, 4 h). Following that, the supernatants were discarded, and 150 µL of DMSO was added to each well to dissolve the MTT formazan crystals and placed on a stirrer (600 rpm, 5 min). Optical absorption was read using an ELISA reader (BIORAD, USA) at 570 nm. The experiment was repeated three times, and the results were compared as a percentage of cells viable in the control well.

Cell viability (%) = Mean OD/Control OD×100%

2.11. Antifungal Activity of TMC-NPs/AmB Against Candida albicans Biofilms

Initially, a suspension containing 10^6 CFU of *Candida albicans* ATCC 10231 (Razi Vaccine and Serum Research Institute, Karaj, Iran) was prepared and 100 µL of it was loaded to 96-well microplates. Then, 100 µL of SDB medium was added and stored (37°C, 48 h). In the next step, the medium containing planktonic cells was discarded and washed three times with PBS. Mature biofilm was exposed to the AmB-sol and TMC-NPs/AmB with concentrations of 0.06 to 16 µg/mL (37°C, 24 h) in three replicates. In this concentration range, biofilm wells were treated with a solution without a drug and used as the control treatment. The two-way ANOVA analysis method was used in order to study the difference between the antifungal activity of AmB-sol and TMC-NPs/AmB (1).

3. Results

3.1. Structural Analysis

The FTIR spectrum of chitosan (Figure 1) shows that the spectral pattern from 500 to 890 cm^{-1} is in the chitosan fingerprint region. The absorption picks in 1035 to 1156 cm^{-1}, 1380 cm^{-1}, 1653 cm^{-1}, 2878 cm^{-1}, and 3433 cm^{-1} are related to the stretching vibrations of the C-O bond of chitosan, C-H bond in the form of methylene CH2, N-H bond in the form of amino NH2, and hydroxyl O-H group bond, respectively. The TMC was synthesized via establishing a reaction between chitosan; moreover, CH3I and its structural changes were studied using the FTIR spectrum. The FTIR spectrum of TMC provides evidence for the occurrence of methylation especially in the region 1200 to 1700 cm^{-1} (Figure 1). The peaks due to angular deformation of N-H bond of amino groups occur in both spectra (1500 to 1620 cm^{-1} for chitosan and at 1559 cm^{-1} for

TMC); however, it is weaker or disappears due to the occurrence of N-methylation. There are peaks at about 1415 to1430 cm^{-1}, which are assigned to the characteristic absorption of N-CH3. Characteristic peaks of alcohol and second alcohol between 1160 and 1030 cm^{-1}, if do not change, confirm the lack of the introduction of an alkyl group at C-3 and C-6 in the chitosan.

3.2. Evaluation of ^{1}H-NMR Spectrum of Synthesized TMC and Methylation Degree

The ^{1}H-NMR spectrum of TMC is shown in Figure 2. The picks available in 1.6 to 2, 2.8 to 3.3, and 4.5 to 5.5 ppm are for a proton of single -NH, as well as -CH and NH-CH3 groups, and hydroxyl O-H group, respectively. The DQ% was calculated at 36.4 in this study.

3.3. AmB Assay

The absorption spectrum of AmB-sol was prepared in a wavelength range of 200 to 900 nm. The AmB-sol showed the maximum absorption at 400 nm. The spectrophotometry in 410 nm was used for measuring the quantity of AmB. The standard calibration curve of AmB in 410 nm prepared in this study is depicted in Figure 3.

3.4. TMC-NPs Characteristics

In the first step, different concentrations and volumetric ratios of TMC and STPP were assessed to determine the optimal conditions for the formation of TMC-NPs with desirable features (e.g., suitable size and surface charge). The TMC-NPs were prepared by TMC (1.8 mg/mL) and STPP solutions (0.6 mg/mL). Furthermore, the volumetric ratio of 5:2 resulted in desirable characteristics (particle size 210±15 nm, PDI 0.30, and ZP +34±0.5 mV), compared to other tested ratios (Table 1). Therefore, this formulation process was regarded as the optimal condition. The SEM images of TMC-NPs prepared in this condition are presented in Figure 4, which exhibited a smooth spherical shape.

3.5. TMC-NPs/AmB Characteristics

The mean particle size of the TMC-NPs/AmB produced at optimal condition was 365±10 nm; moreover, the surface potential and PDI were obtained at +28±0.5 mV and 0.4. In addition, the LE and LC of TMC-NPs/AmB were 76% and 74.04% W/W, respectively. The SEM images of TMC-NPs/AmB that are shown in Figure 5 demonstrate a smooth spherical shape.

3.6. In-vitro Release Study of the Drug from TMC-NPs/AmB

The evaluation of AmB release from TMC-NPs showed that 71% of entrapped AmB were released during 86 h after incubation in a three-step approach. In the first step, an initial burst release of 27% was observed after 8 h. In the second step, a fast release of drug about 13% (range: 27%-40% in the graph) occurred between 8 and 12 h. In the third step, a 36% slow drug release (range: 40%-76%) occurred between 12 and 84 hours (Figure 6). The evaluation of the release profile of TMC-NPs/AmB with various release kinetic models is presented in Figure 7. This figure shows the diffusion mechanism of the drug release that is best explained by the Higuchi kinetics pattern (R^2=95%).

3.7. Drug Potency

The results from the microbiological potency analysis of TMC-NPs/AmB, compared to standard AmB, are shown in Table 2. This potency was analyzed to be 110% using relevant equations.

3.8. Cytotoxicity Test

The cytotoxicity of TMC-NPs/AmB and AmB-sol were determined in the concentration range of 8 to 128 µg/mL on the Vero cells. No toxic effects were observed for both samples with the dilutions of 8 to 16 µg/mL. The cytopathic effects of both samples beginning at a concentration of 32 µg/mL were estimated at 12% and 4% for AmB-sol and TMC-NPs/AmB, respectively. Moreover, at the concentrations of 64 and 128 µg/mL, the cytopathic effects were 41% and 64% for the AmB-sol and 13% and 42% for TMC-NPs/AmB, respectively. The half-maximal inhibitory concentration (CT50) of the AmB-sol and TMC-NPs/AmB were calculated at 105 and 86 µg/mL, respectively (Figure 8).

3.9. Antifungal Activity of TMC-NPs/AmB Against Candida albicans Biofilms

The results from this study demonstrated that drug delivery through developed TMC-NPs has significantly improved the ability of AmB to reduce growth and fungal metabolic activity of *Candida albicans* biofilm (Figure 9). The MIC 50% were estimated at 0.65 and 1.75 μg/mL for TMC-NPs/AmB and AmB, respectively. Furthermore, the MIC 80% for TMC-NPs/AmB and AmB were obtained at 1.95 and 7.75 μg/mL, respectively. TMC-NPs/AmB showed significantly greater antifungal ability, compared to AmB-sol in a similar dosage (P<0.001).

Table 1. Characteristics of different TMC-NPs formulations

Formulation	TMC (mg/mL)	STPP (mg/mL)	Size (nm)	ZP (mV)	PDI
F1	2.0	1.00	1100±15	+16.4±0.5	0.48
F2	2.0	0.75	485±15	+12±0.5	0.32
F3	1.8	0.60	210± 15	+34±0.5	0.30

TMC: Trimethyl chitosan
STPP: Sodium tripolyphosphate
ZP: Zeta potential
PDI: Polydispersity index

Table 2. Results of the TMC-NPs/AmB potency test

St	Conc. ug/mL	Average	SD	RSD %	St	Conc. ug/mL	Average	SD	RSD %	Mean
		16.44	0.76	4.67	**S5**	**1.55**	17.94	0.68	3.80	17.83
		16.00	0.69	4.32	**S4**	**1.25**	17.16	0.61	3.56	17.38
S3	**1**	16.50	0.79	4.79	**S2**	**0.8**	15.83	0.6	3.86	15.66
		16.77	0.97	5.97	**S1**	**0.64**	14.94	0.72	4.86	15.00
Correction point			**0.80**		**Correction point**				**0.65**	
U3	**1**	16.61	0.92	5.58	**S3**	**1**	16.44	0.68	4.14	16.16

TMC: Trimethyl chitosan

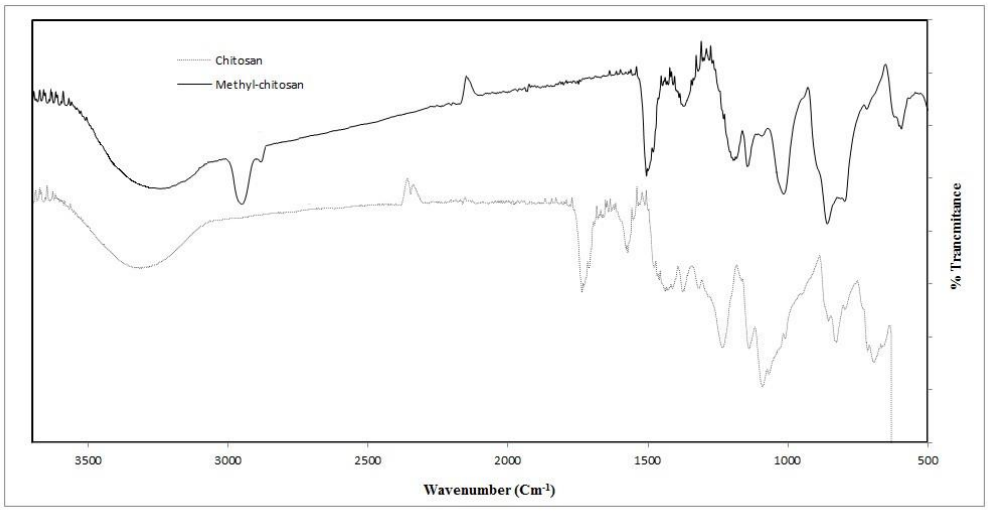

Figure 1. FTIR spectrum of chitosan and TMC
FTIR: Fourier transform infrared
TMC: Trimethyl chitosan

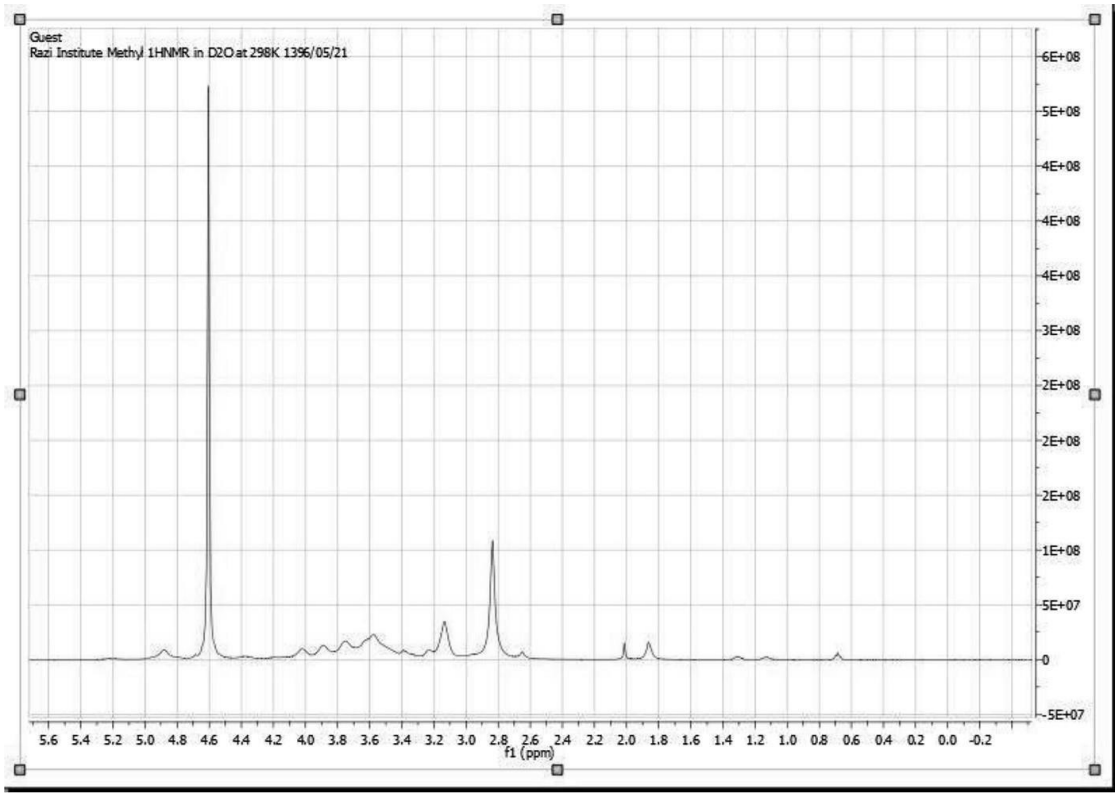

Figure 2. 1H-NMR spectrum of TMC
1H-NMR: Proton nuclear magnetic resonance
TMC: Trimethyl chitosan

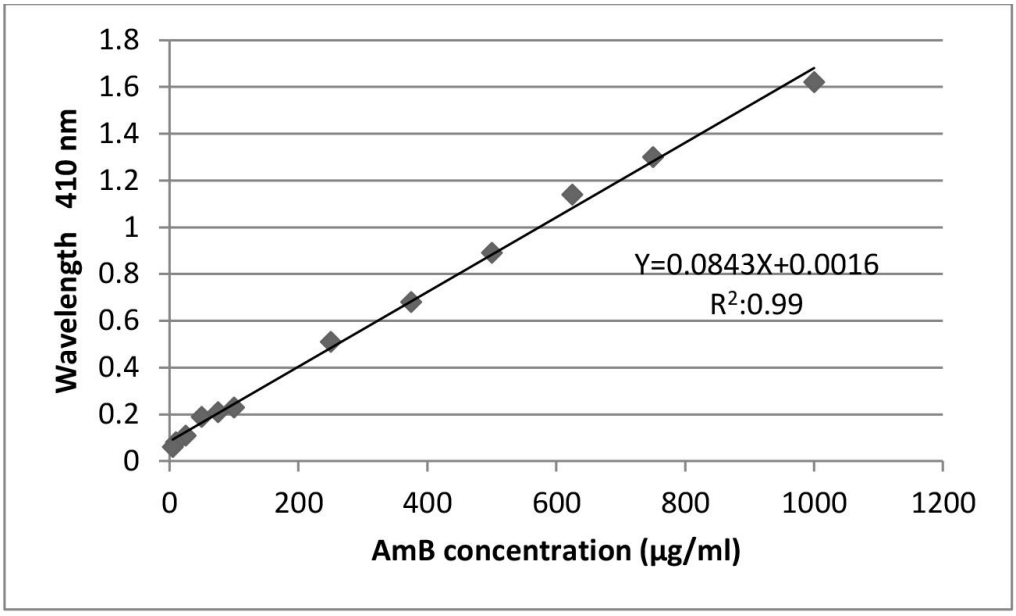

Figure 3. Standard curve of AmB at 410 nm (n=3)

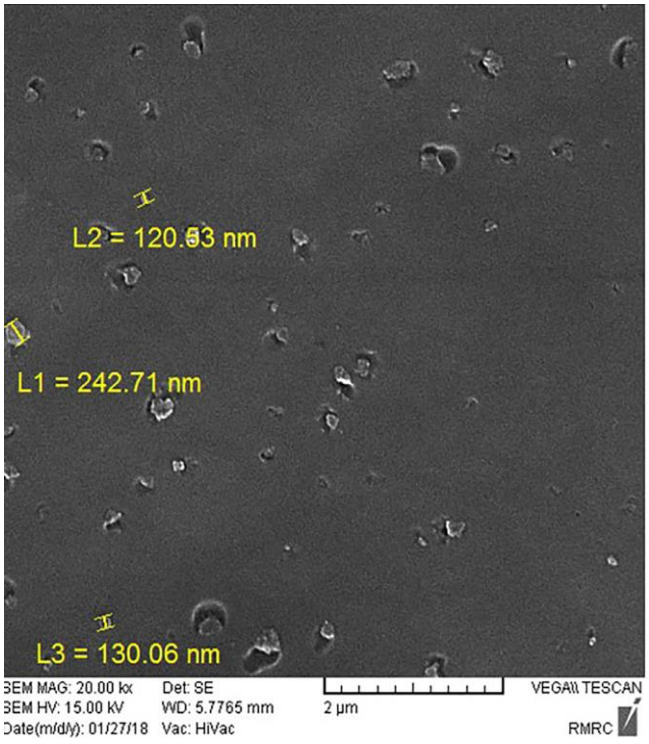

Figure 4. SEM image of TMC-NPs prepared in optimized conditions (TMC solution 1.8 mg/mL, STPP 0.6 mg/ml, and TMC to STPP solutions volume ration 5:2)
SEM: Scanning electron microscopy
TMC-NPs: Trimethyl chitosan
STPP: Sodium tripolyphosphate

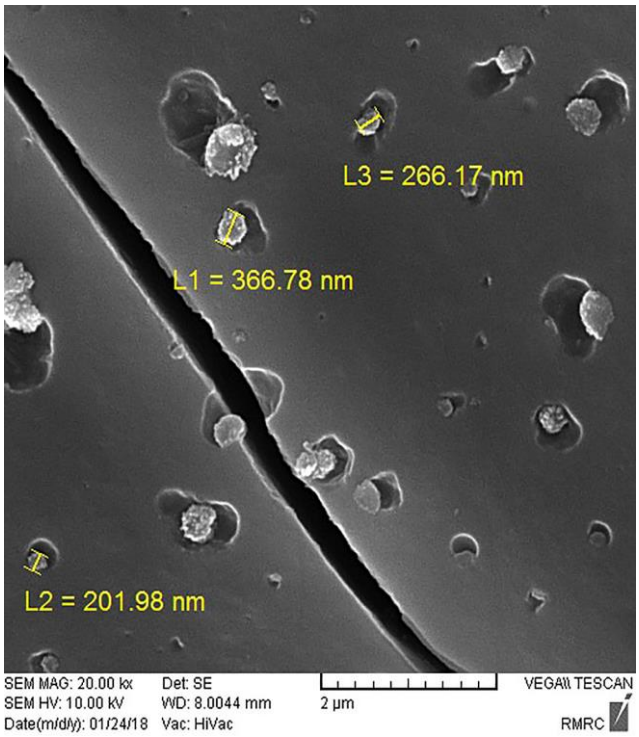

Figure 5. SEM image of TMC-NPs/AmB prepared in optimized conditions. (TMC solution 1.8 mg/mL, STPP 0.6 mg/ml, and TMC to STPP solutions volume ration 5:2)
SEM: Scanning electron microscopy
TMC-NPs: Trimethyl chitosan
STPP: Sodium tripolyphosphate

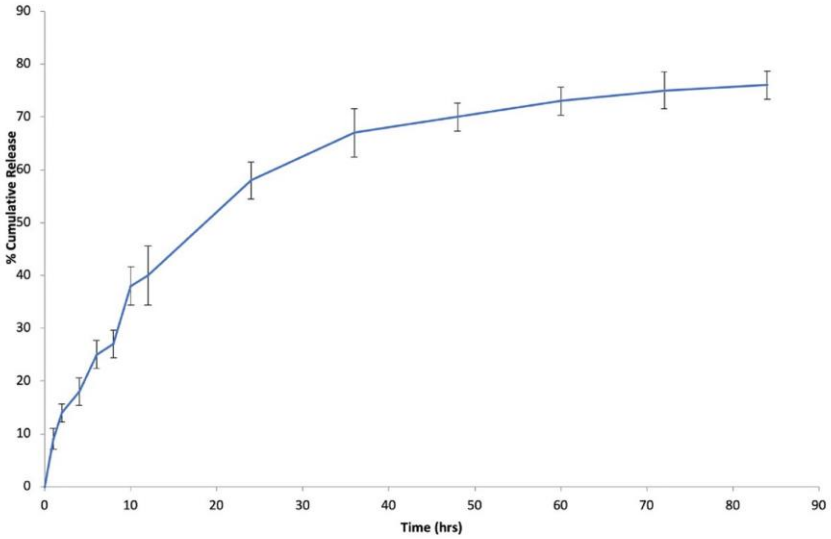

Figure 6. In-vitro release profile of drug from TMC-NPs/AmB prepared under optimized conditions (TMC solution 1.8 mg/mL, STPP 0.6 mg/ml, and TMC to STPP solutions volume ration 5:2) in PBS (pH 7.4, 37 0C) (n=3)
TMC-NPs: Trimethyl chitosan
STPP: Sodium tripolyphosphate
PBS: Phosphate buffer saline

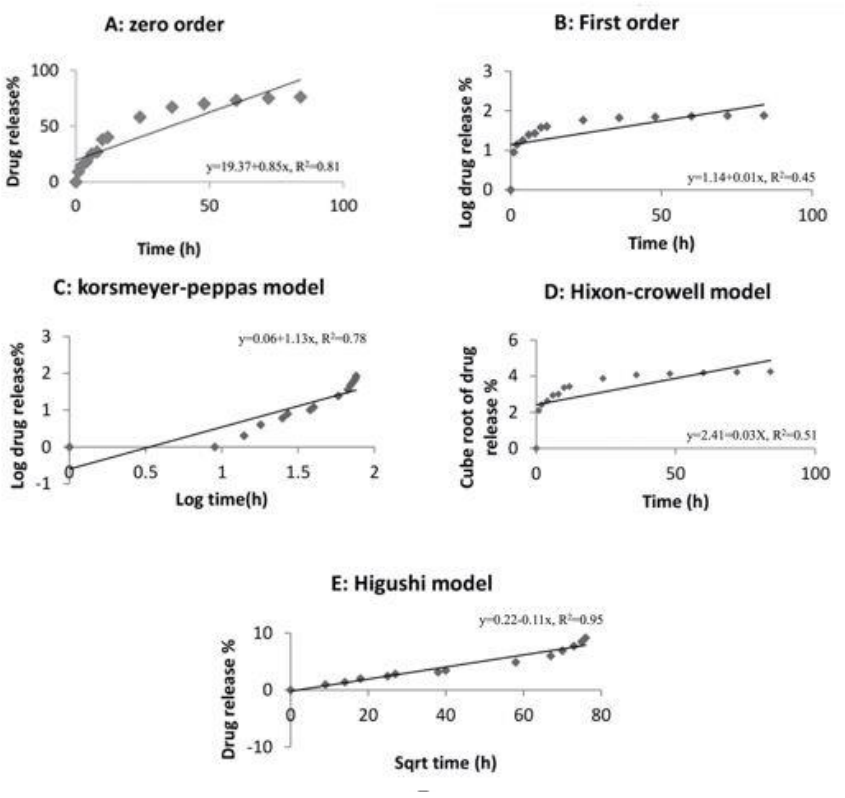

Figure 7. Different release kinetic models of AmB from TMC-AmB/NPs. A: Zero order; B: First order; C: Korsmeyer-Peppas model; D: Hixson-Crowell model, and E: Higuchi model
TMC: Trimethyl chitosan

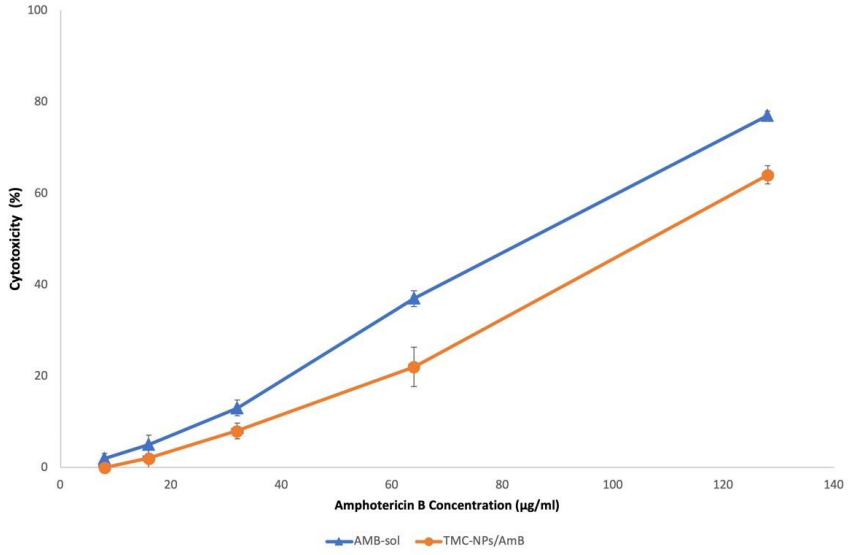

Figure 8. Cytotoxicity results of TMC-NPs/AmB and AmB-sol on Vero cells, as well as AmB concentrations 8-128 µg/mL (n=3)
TMC: Trimethyl chitosan

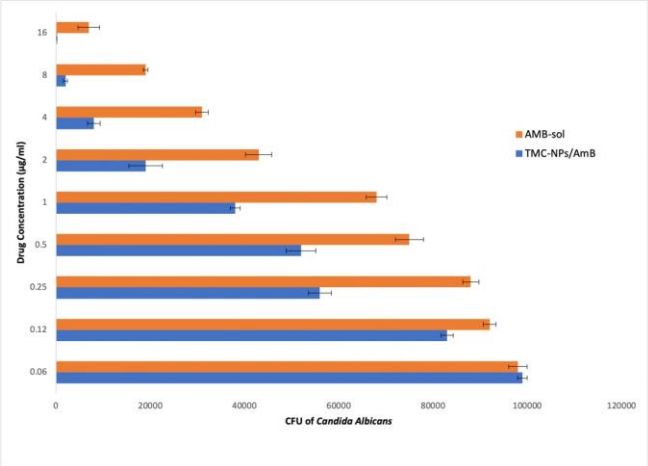

Figure 9. Effects of TMC-NPs/AmB and AmB-sol on the growth rate of Candida albicans biofilm (n=3)
TMC: Trimethyl chitosan

Discussion

During the past decades, AmB has been used as a broad-spectrum antifungal medicine without raising significant concerns with antimicrobial resistance. However, a number of drawbacks are associated with the application of conventional AmB formulations. Several studies have sought to develop modified AmB formulations with a variety of application and delivery methods to overcome these drawbacks (18). Despite the worldwide efforts on improving AmB formulations and drug delivery system, the use of this drug is limited due to its numerous side effects, which indicates a significant gap in research on the development of an efficient and practical formulation (1).

Evidence suggests that delivering AmB through polymeric NPs allows more efficient use of the medicine by lowering the required dose for treatment and delivering the therapeutic agents to the target tissues (22). Therefore, in this study, an ionic gelation technique was developed to prepare chitosan-based TMC-NPs/AmB to improve the antifungal activity of AmB. This technique facilitates a controllable electro-static reaction between cross-linked anionic and polymer cationic groups and allows producing NPs with desirable size and surface charge. The NPs characteristics can be adjusted by changing the process condition to create smaller particles with suitable ZP (23).

The AmB is a water-insoluble agent that precipitates in an acidic medium and dissolves in the alkali mediums. On the other hand, chitosan is insoluble in alkali mediums. Unlike chitosan, the TMC derivative of chitosan is soluble in a broad range of pH and has higher anti-microbial activity, compared to chitosan (24). The TMC can easily be absorbed in the intestine; in addition, it plays an effective role in the protection of drugs that are unstable in the acidic environment of the stomach for oral administration (24). In comparison with chitosan, the higher density of the positive charge of TMC allowed to apply a lower concentration of TMC to prepare NPs. This is caused by ammine groups, compared to chitosan which results in the formation of a stronger electro-static reaction with a cross-linker.

The functional properties of TMC are significantly affected by the methodology applied for the preparation of this molecule (25). There are three methods to synthesize TMC (i.e., one-step, two-step, and three-step). The produced TMC through the one-step method has low water solubility and low quaternization. The resultant polymer from the three-step method has a higher DQ% (more than 80) due to complete O-methylation. The increase in methylation can reduce particle size and ZP. However, this method decreases the available hydrogens for forming hydrogen bonds, which results in the reduction in water solubility of the synthesized TMC. In addition, higher DQ% reduces the rate of TMC encapsulation of the medicine, which is in contrast with the results derived from the one-step and three-step methods. The two-step method of NPs preparation showed preferred TMC properties due to a lower DQ% and higher water solubility (19). Therefore, the two-step method was used in this study for synthesizing TMC resulted in a DQ% of 36.4. The results from our study are relatively similar to the observations by (19) where the application of the two-step technique in the preparation of TMC resulted in a DQ% of 40. Particle size is one of the most important features to take into account and has a significant effect on the efficiency of drug delivery, drug transmission system in penetrating tissue, and effective release of medical factors. Results from a number of other studies have demonstrated that the utilization of a low molecular weight TMC will result in the preparation of smaller NPs sizes (26).

In this study, low molecular weight TMC was synthesized for TMC-NPs preparation to minimize the NPs size. The FTIR spectrum of chitosan and TMC (Figure 1) showed peaks at 3012 cm^{-1} to 3129 cm^{-1}, which correspond to C-H bond vibrations in the presence of the methyl-CH3 group. The presence of CH3-methyl is the evidence of the methylation of chitosan. The ^{1}H-NMR structural study of TMC demonstrated a 36% methylation value (Figure 2). This result is similar to the findings obtained by Farhadian, Dounighi (14) that observed a 40% degree of quaternization in the TMC preparation process at the peak appointment and intensity.

The STPP is basically a food additive that has been widely applied as a biocompatible cross-linker in NPs synthesis. In addition, it has been observed that STPP may have antifungal effects. Therefore, in this study, STPP as a negatively charged molecule was used as a cross-linker to improve the anti-fungal effects of the drug. By increasing the ratio of chitosan molecular weight to STPP and concentration of chitosan in solution, the viscosity of the whole solution increases. As a result, the resistance of the liquid phase against dispersion increases which leads to the formation of larger NPs. This increase in STPP concentration in the solution causes the aggregation of the NPs and increases in particle size (19).

The amount and procedure of STPP utilization in NPs preparation has a direct effect on particle size and its ZP (27). Valuable efforts have been made by previous studies to find the optimal condition and best ratio of STPP to chitosan that results in smaller NPs preparation. Xu, Xu (17) observed that the phase ratio of 10:1.8 between STPP (1 mg/mL) and TMC solutions (1 mg/mL, pH 7.4) at a 200 rpm stirring rate minimized the particle size. Their methodology resulted in the preparation of NPs with the mean particle size was 250±50 nm and ZP of +14.6±0.8 mV. In another study, the minimum particle size of NPs was obtained at the phase ratio of 10:2 TMC to HPMC (as a cross-linker) and constant shaking of 1000 rpm (TMC: 1 mg/mL, HPMC: 1 mg/mL,) which resulted in mean NPs size of 85±10 nm (14).

Therefore, to optimize the TMC to STPP volume ratio in this study, ratios close to the previous successful studies were tested. The optimum TMC to STPP volume ratio that resulted in minimized TMC-NPs size was achieved at 5:2. Furthermore, the prepared TMC-NPs at optimized conditions (TMC: 1.8 mg/mL, STPP: 0.6 mg/mL, and TMC to STPP volume ratio 5:2) resulted in a mean particle size of 210±15

nm, PDI of 0.30, and ZP of +34±0.5 mV (Table 1) and relatively smooth spherical shape observed in SEM image (Figure 4). The TMC-NPs/AmB prepared at optimal conditions of this study (TMC: 1.8 mg/mL, STPP 0.6: mg/mL, and TMC to STPP volume ratio of 5:2) showed the mean particle size 365±10 nm, PDI of 0.4, ZP of +28±0.5 mV, LE of AmB 76% W/W, LC 74.04% W/W, and a smooth spherical shape in SEM image (Figure 5).

In this study, the *in vitro* release profile of the TMC-NPs/AmB (Figure 6) showed two major three phases. In the initial phase, the burst release of about 27% of AmB was released with a constant speed during the first 8 h. This phase was due to the presence of the drug on the surfaces of TMC-NPs/AmB that enables the drug to rapidly enter its surrounding media. In the second phase, which occurred between 8 and 12 hours, a fast release of drug was observed, and 13% (range of 27 to 40% in the graph) of the drug was released in this phase. In the third step, 36% of drugs that were released slowly (range: 40%-76%) occurred between 12-84 h. In this step, the AmB was released from TMC-NPs due to the penetration of water, swelling, and erosion of TMC-NPs.

Through this process, 76% of the entrapped drug is released up to 84 h. This observation proved that the technique used in this study could significantly reduce the speed of drug release in comparison with a number of previous reports. Zarifpour, Hadizadeh (19) showed that the use of TMC with a DQ% of 40% for the preparation of NPs depicted a shorter drug release time reaching its maximum level within 3 h, which then continued with a constant rate for 4 h.

Some other factors, such as the composition of NPs, NPs fabrication method, and NPs specifications, can also have a significant effect on drug release behaviors. In a previous study AL-Quadeib, Radwan (18), a fine particle (particle size of 50 nm) containing AmB prepared by using PLGA showed a rapid drug release, and almost 60% of the drug was released within the first 24 h. Xu, Xu (17) indicated that 6.5% of vancomycin was released from NPs with a mean particle size of 220 nm within 24 h, where the release process was controlled for 32 h.

The drug release from our TMC-NPs/AmB was evaluated for the first-order, zero-order, Hixon-Crowell, Higuchi, and Korsmeyer-Peppas model's kinetics. Our results showed (Figure 7) that the drug release from TMC-NPs/AmB best fitted with Higuchi kinetic model (R^2=0.95). Therefore, the evaluation of release kinetics reveals that both diffusion and erosion mechanisms contribute to the release process.

The results from the cytotoxicity test on Vero cells showed that the CT50 of AmB-sol and TMC-NPs/AmB were 105 and 86 μg/mL, respectively. These results suggest a significantly ($P<0.05$) lower toxicity of TMC-NPs/AmB in comparison with AmB-sol at the same antibiotic dosage. The lower toxicity and improved biocompatibility of TMC-NPs/AmB could be caused by reducing the oxidative stress in the cells. Oxidative stress disrupts intracellular homeostasis by interacting with cellular macromolecules. Similar cytotoxicity results were obtained by Xu, Xu (17) using AmB NPs and chitosan.

The antifungal performance of the developed TMC-NPs/AmB was tested in comparison with AmB-sol using doses of 0.125, 0.25, 0.5, and 1.0 μg/mL. At the concentration of 0.25 μg/mL, the TMC-NPs/AmB resulted in a 32% higher reduction of fungal biofilm metabolic activity, compared to the traditional drug delivery system. The greatest difference was observed at the concentration of 1 μg/mL in which the TMC-NPs/AmB reduced fungal biofilm metabolic activity and AmB-sol about 62% and 32%, respectively ($P<0.001$).

At higher concentrations (e.g., 8 and 16 μg/mL), no statistically significant difference was observed between the two drugs ($p>0.05$). These results suggest that TMC-NPs/AmB could potentially affect the permeability of the extracellular polymeric matrix that is secreted by biofilms. In addition, unlike the short treatment durability of the traditional drug system, TMC-NPs/AmB provides suitable and longer effect durability. Therefore, it is foreseeable that by using

TMC-NPs/AmB, the inhibition of fungal growth is possible via a lower dose of AmB. This can prevent the need for increasing the total drug dose and the development of drug resistance.

The nano-drug delivery system has several advantages, compared to the traditional drug delivery methods, such as higher stability, enhanced bioavailability, feasibility of variable routes of administration, side effect reduction, controlled release upon transferring, and localization of target tissue over the traditional delivery mechanisms. Inattention to these advantages and results of the present study, the novel TMC-NPs/AmB developed in this study has clinical applicability potential that can be a desirable alternative capability for traditional drug delivery systems.

The main objective of this study was to develop a novel TMC-NPs formulation to improve AmB delivery performance in order to decrease the dose of the drug and minimize the adverse effects, which was successfully achieved. A low-molecular-weight TMC was synthesized for TMC-NPs/AmB preparation. The results from this study also demonstrated that the encapsulation of AmB improved the antifungal activity of the drug and elongated the duration of drug release. This result can potentially decrease the adverse effects associated with the application of the traditional form of AmB by reducing the total required dosage and shortening the duration of antibiotic therapy. A cost-effective procedure was also developed in this study that can be implemented in the pharmaceutical industry for the synthesis of biocompatible TMC-NPs. Therefore, this study suggests a novel TMC-NPs/AmB as a suitable alternative to the traditional AmB delivery system from both biological and practical points of view.

Authors' Contribution

Study concept and design: N. M. D. and M. B.
Acquisition of data: L. N. Sh.
Analysis and interpretation of data: N. M. D. and N. M.
Drafting of the manuscript: N. M. D. and L. N. Sh.
Critical revision of the manuscript for important intellectual content: N. M. D. and M. B.
Statistical analysis: N. M. D. and L. N. Sh.
Administrative, technical, and material support: Razi Vaccine and Serum Research Institute

Ethics

We hereby declare all ethical standards have been respected in preparation of the submitted article.

Conflict of Interest

The authors declare that they have no conflict of interest.

Grant Support

This study was supported by Razi Vaccine and Serum Research Institute, Agricultural Research, Education and Extension Organization.

Acknowledgment

The authors would like to thank the supports of the Razi Vaccine and Serum Research Institute, Karaj, Iran.

References

1. Sanchez DA, Schairer D, Tuckman-Vernon C, Chouake J, Kutner A, Makdisi J, et al. Amphotericin B releasing nanoparticle topical treatment of Candida spp. in the setting of a burn wound. Nanomed-Nanotechnol. 2014;10(1):269-77.
2. Grela E, Zdybicka-Barabas A, Pawlikowska-Pawlega B, Cytrynska M, Wlodarczyk M, Grudzinski W, et al. Modes of the antibiotic activity of amphotericin B against Candida albicans. Sci Rep. 2019;9(1):1-10.
3. Roy G, Galigama RD, Thorat VS, Mallela LS, Roy S, Garg P, et al. Amphotericin B containing microneedle ocular patch for effective treatment of fungal keratitis. Int J Pharm. 2019;572:118808.
4. Dominguez E, Zarnowski R, Choy H, Zhao M, Sanchez H, Nett J, et al. Conserved Role for Biofilm Matrix Polysaccharides in Candida auris Drug Resistance. mSphere. 2019;4.
5. Dominguez E, Zarnowski R, Choy HL, Zhao M, Sanchez H, Nett J, et al. Conserved Role for Biofilm

Matrix Polysaccharides in Candida auris Drug Resistance. mSphere. 2019;4(1):e00680-18.
6. Wang JJ, Zeng ZW, Xiao RZ, Xie T, Zhou GL, Zhan XR, et al. Recent advances of chitosan nanoparticles as drug carriers. Int J Nanomedicine. 2011;6:765-74.
7. Singh G, Kaur T, Kaur A, Kaur R, Kaur R. Analytical methods for determination of Amphotericin B in biological samples: a short review. JABS. 2014;1:R26-R32.
8. Salah R, editor Antileishmanial activities of chitin and chitosan prepared from shrimp shell waste. Int Conf Chem Mettalurgy Environ Eng; 2015.
9. Vongchan P, Wutti-In Y, Sajomsang W, Gonil P, Kothan S, Linhardt RJ. N, N, N-Trimethyl chitosan nanoparticles for the delivery of monoclonal antibodies against hepatocellular carcinoma cells. Clin Microbiol Infect. 2011;85(1):215-20.
10. Wu J, Huang Y, Yao R, Deng S, Li F, Bian X. Preparation and characterization of starch nanoparticles from potato starch by combined solid-state acid-catalyzed hydrolysis and nanoprecipitation. Starch Starke. 2019;71(9-10):1900095.
11. Cakic M, Glisic S, Nikolic G, Nikolic GM, Cakic K, Cvetinov M. Synthesis, characterization and antimicrobial activity of dextran sulphate stabilized silver nanoparticles. J Mol. 2016;1110:156-61.
12. Xu C, Rezeng C, Li J, Zhang L, Yan Y, Gao J, et al. 1H NMR-Based Metabolomics Study of the Toxicological Effects in Rats Induced by "Renqing Mangjue" Pill, a Traditional Tibetan Medicine. Front Pharmacol. 2017;8:602.
13. Perez AP, Altube MJ, Schilrreff P, Apezteguia G, Celes FS, Zacchino S, et al. Topical amphotericin B in ultradeformable liposomes: Formulation, skin penetration study, antifungal and antileishmanial activity in vitro. Colloids Surf B. 2016;139:190-8.
14. Farhadian A, Dounighi NM, Avadi M. Enteric trimethyl chitosan nanoparticles containing hepatitis B surface antigen for oral delivery. Hum Vaccin Immunother. 2015;11(12):2811-8.
15. Wu M, Long Z, Xiao H, Dong C. Recent research progress on preparation and application of N, N, N-trimethyl chitosan. Carbohydr Res. 2016;434:27-32.
16. Ofori-Kwakye K, Mfoafo KA, Kipo SL, Kuntworbe N, El Boakye-Gyasi M. Development and evaluation of natural gum-based extended release matrix tablets of two model drugs of different water solubilities by direct compression. Saudi Pharm J. 2016;24(1):82-91.
17. Xu J, Xu B, Shou D, Xia X, Hu Y. Preparation and evaluation of vancomycin-loaded N-trimethyl chitosan nanoparticles. Polymers. 2015;7(9):1850-70.
18. AL-Quadeib BT, Radwan MA, Siller L, Horrocks B, Wright MC. Stealth Amphotericin B nanoparticles for oral drug delivery: In vitro optimization. Saudi Pharm J. 2015;23(3):290-302.
19. Zarifpour M, Hadizadeh F, Iman M, Tafaghodi M. Preparation and characterization of trimethyl chitosan nanospheres encapsulated with tetanus toxoid for nasal immunization studies. Pharm Sci. 2013;18(4):193-8.
20. Yan C, Hu CQ. Improvement of microbiological potency measurement of amphotericin B. Chinese Antibiot. 2013;38:434-9.
21. Pharmacopoeia U, editor National Formulary.< 81> Antibiotics-Microbial assays. USP32-NF27, US Pharmacopeial Convention Inc, Rockville, USA; 2009.
22. De Jong WH, Borm PJ. Drug delivery and nanoparticles: applications and hazards. Int J Nanomed. 2008;3(2):133.
23. Pant A, Negi JS. Novel controlled ionic gelation strategy for chitosan nanoparticles preparation using TPP-β-CD inclusion complex. Eur J Pharm SCI. 2018;112:180-5.
24. Mourya VK, Inamdar NN. Trimethyl chitosan and its applications in drug delivery. J Mater Sci Mater Med. 2009;20(5):1057-79.
25. Rebelatto MC, Guimond P, Bowersock TL, HogenEsch H. Induction of systemic and mucosal immune response in cattle by intranasal administration of pig serum albumin in alginate microparticles. Vet Immunol Immunopathol. 2001;83(1):93-105.
26. Yien L, Zin NM, Sarwar A, Katas H. Antifungal activity of chitosan nanoparticles and correlation with their physical properties. Int J Biomater. 2012;2012.
27. Chen F, Zhang Z-R, Huang Y. Evaluation and modification of N-trimethyl chitosan chloride nanoparticles as protein carriers. Int J Pharm. 2007;336(1):166-73.